Effect of Heat Transfer on Transonic Flow over an Aerofoil

D. Mitchell and S. Raghunathan
Department of Aeronautical Engineering
Queens University, Belfast, U.K.

Abstract

The effect of the model surface to freestream adiabatic temperature ratio (T_w/T_{ad}) on subsonic flows at zero pressure gradient and transonic flow over a NACA0012 aerofoil are evaluated using a computational fluid dynamic approach. The analysis based on the Thin Layer Navier Stokes Equations with Baldwin Lomax turbulence model indicated that surface heat transfer has significant effects on both subsonic and transonic flows confirming some of the experimental data available. The results have implications in wind tunnel testing at non-adiabatic surface conditions.

Nomenclature

c	model chord length
C_d	aerodynamic drag coefficient
C_l	aerodynamic lift coefficient
C_f	skin friction coefficient
C_p	pressure coefficient
H	boundary layer shape factor δ^*/θ
k	thermal conductivity
M, M_e	free stream, boundary layer edge Mach number
R, R_θ	Reynolds number based on chord length, boundary layer momentum thickness
T_w, T_{ad}	surface, adiabatic recovery temperature
U, U_e	free stream, boundary layer edge velocity
x, y	co-ordinates from the leading edge of model
y^+	normalised distance based on friction velocity
δ	boundary layer thickness
δ^*	boundary layer displacement thickness
θ	boundary layer momentum thickness
α	angle of airflow incidence
ρ	density
μ	viscosity

1. Introduction

Convective heat transfer can have significant influence on the aerodynamics of flow over bodies. Experiments on boundary layers with heat transfer have shown that the boundary layer development[1], laminar or turbulent, boundary layer transition[2,3] and separation on a model surface[4-7] are sensitive to heat transfer between the model and the flow field. It can be inferred from these experiments that cooling ($T_w/T_{ad} < 1$) postpones boundary layer transition and for a turbulent boundary layer produces a fuller velocity profile, increased skin friction, and decreased boundary layer thickness and shape factor. In the case of separated flows cooling also reduces the length of separation bubble. Heating the model ($T_w/T_{ad} > 1$) has the opposite effect to that of cooling. In the case of transonic flow with shock interaction, heat transfer can have a significant and favourable effects on the shock wave boundary layer interaction[4,8,9]. It is envisaged that in transonic flows model cooling can reduce the scale of shock induced separation and improve aerofoil trailing edge pressure recovery.

For an aircraft in free flight the surface temperature of the aircraft is nearly equal to the recovery temperature of the free stream and therefore the heat transfer effects mentioned above may not be of any importance. However in testing a model in short duration facilities and cryogenic wind tunnels where there could be significant differences between the model temperature and the free stream recovery temperature leading to spurious scale effects in measurement of both static and dynamic forces on a model. It has been estimated[10] that an increase in one per cent in model-to-stream temperature ratio has an effect equivalent to that of three and a half per cent reduction in the Reynolds number. It is suggested that some of the scale effects associated with the Reynolds number can be identified by cooling or heating the model relative to adiabatic temperature of the air flow[11]. Recent experiments[12] on biconvex aerofoils with cooling tend to support these suggestions and also have demonstrated that surface cooling has a large effect on dynamic measurements such as buffet.

The above understanding of the effects of heat transfer on flow over aerofoils is based on a limited amount of experimental data, hypothesis and inference.

The aim of this paper is to achieve a further understanding of the effect of heat transfer on subsonic flow over a flat plate and transonic flow over aerofoils by CFD approach. The effect of heat transfer on wind tunnel testing of aerofoils and the possibility of identifying scale effects associated with Reynolds number by model cooling or heating are discussed.

2. CFD Description and Validation

The computational fluid dynamic code was based on two-dimensional time averaged thin layer Navier Stokes equations with a Baldwin-Lomax turbulence model[13]. Sutherland's law was used for viscosity and the Prandtl analogy was employed for thermal conductivity. A cartesian grid with 150 x 50 grid cells with denser cells near the surface was used for the computation of flow over a flat plate. The initial normal spacing was set at $1x10^{-3}$ chords, corresponding to a value of $y^+ \leq 5$ which satisfies the thin layer conditions. The outer boundary was located at 10 chord lengths. The grid used for aerofoil calculations was a C grid (Fig.1) with 300 x 60 grid cells. The outer far field for these calculations was located at 50 chord lengths from the aerofoil surface.

The numerical scheme was the Implicit MacCormack Predictor Corrector finite volume method with cell centred mesh and Gauss-Seidel time relaxation[14]. The upwind flux vector splitting method of Van Leer[15] was used for attenuating the numerical oscillations in the vicinity of shock waves. The continuously differentiable flux limiter proposed by Mulder and Van Leer[16] was used to eliminate undershoots and overshoots in the shock region. Farfield boundary conditions were imposed implicitly. The surface boundary conditions were implicit for adiabatic wall conditions and explicit for non-adiabatic wall conditions. Flow variables at the wake cut were calculated as the average linear extrapolation from above and below the cut.

Calculations for the flat plate were made with an initial 20 iterations on a coarse grid and 60 iterations on a fine grid. For the aerofoil 50 iterations were performed on the coarser grid before the converged solution was transferred to the fine grid. The full convergence to a steady state solution was obtained after approximately 250 iterations on the finer grid.

The code was validated against standard cases for NACA0012 and RAE2822 aerofoils. Figure 2 shows typical validations. Fig.2a shows the code validation for pressure distribution for RAE2822 $M=0.73$, $R=6.5x10^6$, $\alpha=2.79°$ at adiabatic surface conditions Navier D refers to the design co-ordinates. Navier M and circles refer to the measured co-ordinates and experimental data of Cook et al[17] respectively. Transition was fixed at 3% chord on both the upper and lower surfaces. The measured aerofoil pressure distribution compares favourably with the experimental results. Small differences in the pressure distribution between the experimental data and computation near the leading edge and the shock interaction region have also been observed by other authors. The differences in C_p near the leading edge may be attributed to the experimental errors associated with the transition tipping. The differences in C_p in the shock interaction region is due to the inability of the turbulence model to predict correctly the shock boundary layer interaction. The computed values of δ^* and θ on the upper surface of the aerofoil for the above test case also compared favourably with the experimental results.

Figure 2b shows the pressure distribution on a NACA 0012 aerofoil at $M=0.7$, $R=9x10^6$ and $\alpha=2.57°$ with transition fixed at 5% chord, a case corresponding to a fully attached and sub-critical flow over an aerofoil. The agreement between the computed and experimental results is very good.

Figure 2c shows a severe test case for validation of the code; pressure distribution on a NACA0012 aerofoil at $M_\infty=0.79$, $R=9x10^6$ and $\alpha = 2.57°$. Transition was fixed at 5% chord. The discrepancy between the experimental and computational results for shock position and the pressure distribution in the shock wave boundary layer interaction region have also been observed by Maksymiuk and Pulliam[18] and others. These have been attributed to the inadequacy of the turbulence models for transonic flows with strong interactions.

The lift-drag polar for NACA0012 aerofoil at $M=0.7$ and $R=9x10^6$ based on the computational results are compared with the experimental and computed results of Harris[19] and ARC2D[18] respectively in figure 2d. The transition was fixed at 5% chord for all these results. The computed results compare very favourably with the other results.

A validation of the code for heat transfer is shown in figure 2e. In this figure the computed and experimental values[20] of the Stanton number are plotted against R_θ for a flat plate at $M=1.69$, $R=10^6$ and $T_w/T_{ad}=1.65$. The Spalding-Chi correlation[21] based on computed values of the Stanton number and skin friction are also included in this figure. The agreements between the computed results and the experimental data are good at higher values of R_θ indicating that the numerical code can predict heat transfer with reasonable accuracy at higher R_θ values ($R_\theta \geq 6000$).

3. Heat Transfer Effects on Flat Plate Boundary Layer

Results of the computation of subsonic flow over a flat plate (zero pressure gradient) are shown in figures 3 and 4. Figure 3 refers to a laminar boundary layer on a flat plate at M=0.5, R=$8x10^3$ and T_w/T_{ad}=0.6, 1.0 and 1.4. The effects of heat transfer on a laminar boundary layer at zero pressure gradient are appreciable.

Surface cooling increases the velocities (Fig.3a) and momentum of the air flow (Fig.3b) within the boundary layer. Surface heating has the opposite effect to that of cooling. The trends in velocity profiles are similar to those measured by Van Driest[1]. It has also been observed by Back and Cuffel[22] that the momentum of the boundary layer near the surface increases with cooling and decreases with heating.

Figures 3c to 3f refer to the values of the boundary layer thickness, displacement thickness, shape factor and skin friction respectively. In these figures the values are normalised with respect to the corresponding values at adiabatic wall conditions and are plotted against temperature ratio for the above case. The general effect of cooling is to decrease δ (Fig 3c), δ^* (Fig.3d), H (Fig 3e) and increase C_f (Fig 3f).

The effect of heat transfer on a turbulent boundary layer at zero pressure gradient is typified in Figure 4. The results shown here are for the velocity (Fig.4a) and momentum (Fig.4b) profiles at M=0.5, R=$1x10^6$ and T_w/T_{ad}=0.6, 1 and 1.4. The effect of heat transfer on the velocity profile is not as large for a turbulent boundary layer at zero pressure gradient as that noticed for laminar boundary layers. However, as was the case for the laminar boundary layer the effect of heat transfer on the momentum profile is significant.

The observed results here can be traced to the effect produced by the temperature of the wall relative to the adiabatic temperature on the viscosity, density and energy exchange of the air near the surface. To illustrate the reasons for the effects observed the cold wall case is considered. A cold wall would result in a transfer of energy within the boundary layer and towards the wall resulting in an increase in the velocities near the wall and velocity gradients normal to the surface. The air near the cold wall also has a relatively higher density. The combined effect of increase in ρ and u near the wall leads to a large increase in mass and momentum flow. The displacement thickness is primarily controlled by the mass flow near the wall and therefore decreases with cooling. The fuller velocity profile leads to a decrease in the shape factor.

The skin friction, C_f is proportional to $\mu du/dy$. Model cooling decreases μ and increases du/dy. The fact that C_f increases with a reduction in wall temperature indicates that for a zero pressure gradient boundary layer the effect of cooling on the velocity gradients near the wall are larger than those due to viscosity.

The exchange of momentum and energy in a laminar boundary layer at adiabatic wall conditions is due to molecular motion. The velocity profile is not as full as the turbulent profile where the exchange of momentum and energy takes place by turbulent eddies. The effect of model cooling on the laminar velocity profile is to make it fuller leading to large changes in the boundary layer profile and its integral values.

The effect of heat transfer on a turbulent velocity profile and therefore the velocity gradients near the wall is relatively small due to the fact that the energy changes produced by heat transfer are only a small proportion of the energy exchange produced by the turbulent motion.

In general some of the effects observed here due to surface cooling on a flat plate boundary layer are analogous to that of boundary layer suction in the sense that boundary layer suction also produces a transfer of energy in the boundary layer towards the surface leading to a fuller velocity profile, increased velocity gradients, increased skin friction and decreased the shape factor. However, unlike boundary layer suction cooling decreases the viscosity and increases the density near the surface resulting in a considerable increase in the "effective" Reynolds number.

The effects of heating on the boundary layer are generally opposite to that of cooling.

4. Heat Transfer Effects on Transonic Flow Over an Aerofoil

The effects of heat transfer on transonic flow over a NACA0012 aerofoil can be observed from figures 5 to 7. Figure 5 refers to subcritical flow over the aerofoil at M=0.7, R=$9x10^6$ and α=0°, and for T_w/T_{ad}=0.6, 1, 1.4. Figure 6 refer to super critical flow with shock induced separation at M=0.85, R=$9x10^6$, α=0° and for T_w/T_{ad}=0.6, 1, 1.4. Transition was fixed at 5% chord for both cases.

At sub critical conditions heat transfer has only a small effect on the surface pressure distribution (Fig.5a). The effect of cooling on the surface pressure distribution is to decrease the pressures and increase the local Mach numbers. The effect of heating on the surface

pressures is even smaller than produced by cooling. Similar observations at subcritical flows have been made by Inger[8]. The effect of heat transfer on drag is significant (Fig.5b). At adiabatic conditions the pressure drag and skin friction drag are of the same order. Cooling has negligible effect on the pressure drag but reduces skin friction and therefore the total drag.

The pressure distribution on the surface of a NACA0012 aerofoil at super critical conditions (Fig.6a) indicate that surface cooling moves the shock rearwards, increases the shock strength and improves the pressure recovery at the trailing edge. The pressure gradients in the shock interaction region are increased. Cooling increases the Mach numbers (Fig.6b) and momentum (Fig.6c) within the boundary layer and decreases the displacement thickness (Fig.6d) and skin friction (Fig 6e). Similar effects of cooling on transonic flows have been observed experimentally

The effects observed here are due to the effect of heat transfer on the boundary layer thickness and sonic height which in transonic flows are of the same order. The rearward movement of the shock wave may be attributed to the reduced displacement thickness of the boundary layer approaching the shock wave. The increased shock strength and pressure gradients in the shock interaction region are due to a reduction in the sonic height and a corresponding reduction in the communication across the shockwave . These are evident by the Mach number profiles (Fig.6b) and momentum profiles (Fig.6c) at three chordwise positions namely; upstream of the shock (x/c=0.6), downstream of the shock (x/c=0.75) and close to the trailing edge (x/c=0.90) and the variation of displacement thickness in the chordwise direction (Fig.6d).

The skin friction values on the surface of the aerofoil surface (Fig.6e) indicate that for the adiabatic case the flow is separated downstream of the shock wave. The effect of model cooling is to decrease C_f in the region of negative pressure gradients. In this region the effect of cooling on the mass flow profile and therefore the velocity profile is negligible, largely due to the transfer of energy towards the surface due to turbulent eddies far outweighing the heat transfer effects. (The velocity profile is very full at adiabatic surface conditions.) The major effect of cooling on the skin friction is through viscosity which decreases with cooling, that is C_f decreases with reduced surface temperature.

The fact that surface cooling improves the pressure recovery near the trailing edge of the aerofoil indicates that cooling also reduces the height of the separation bubble as can be observed from the δ^* values in the separated region. This may be attributed to the increase in momentum of the boundary layer approaching the shock wave (Fig.6c).

Figure 7 shows the effect of heat transfer on the lift and drag coefficients for a NACA0012 aerofoil at $M=0.7$, $R=9\times10^6$, $\alpha=0$ to 5° and $T_w/T_{ad}=0.6$, 1 and 1.4. For a given incidence surface cooling increases the lift coefficient, C_l (Fig.7a), this being more noticeable at higher values of incidence. The increase in lift is associated with the increased velocities on the surface. Surface cooling also reduces the overall drag coefficients due the effects on the boundary layer discussed earlier. Thus there is an increase in the lift to drag ratio (Fig.7b) and improvement in the performance of the aerofoil. The effect of heating is opposite to that of cooling. These results are in agreement with the experimental results of Macha et al[4] at low speeds.

All the results presented here indicate that surface heat transfer can introduce spurious scale effects in wind tunnel testing as observed by Green et al[10]. Further, the effects of cooling on the flow over an aerofoil are similar to those produced with an increase in Reynolds number. Therefore, it may be possible to identify scale effects associated with Reynolds number by cooling or heating the model relative to the adiabatic temperature.

5. Conclusions

The effect of heat transfer on steady subsonic and transonic flow may be summarised as follows.

Model cooling:

(i) produced a thinner boundary layer,
(ii) increased the momentum within the boundary layer,
(iii) increased shock Mach number and pressure gradients in the shock interaction region,
(iv) produced a rearward movement of the shock wave,
(vi) reduced the height of the separated flow, and
(vii) increased pressure recovery at the trailing edge.

Surface heating produced opposite effects to cooling.

Testing a model in a wind tunnel at non-adiabatic surface temperatures can lead to spurious scale effects.

Heat transfer may be a technique which could be used to identify scale effects on models.

6. References

1. Van Driest, E.R., "Convective Heat Transfer in Gases", In: turbulent Flows and Heat Transfer in High Speed Aerodynamics and Jet Propulsion, Section F. Vol. 5, Oxford University Press, 1969.

2. Dougherty, N.S. and Fisher, D.F., "Boundary Layer Transition on a 10° Cone: Wind tunnel and Flight Test Correlation", AIAA paper 80-01544, 1980.

3. Liepmann, H.W. and Fila, G.H., "Investigations of Effect of Surface Temperature and Single Roughness Elements on Boundary Layer Transition", NACA TN 1196, 1947.

4. Macha, J.M., Norton, D.J. and Young, J.C. "Surface Temperature Effects on Subsonic Stall", AIAA paper 72-960, 1972.

5. Lynch, F.T., Faucher, M.F., Patel, D.R. and Inger, G.R., "Adiabatic Model Wall Effects on Transonic Airfoil Performance in Cryogenic Wind Tunnels", AGARD CP 348, paper 14, 1983.

6. Frishett, J.C., "Incipient Separation of a Supersonic Turbulent Boundary layer Including Effects of Heat Transfer", PhD Thesis, University of California, 1971.

7. Elfstrom, G.M., "Turbulent Separation in Hypersonic Flow", Imperial College of Science and Technology, Aero. Report 71-16, 1971.

8. Inger, G.R., Lynch, F.T. and Faucher, M.F., "A Theoretical and Experimental Study on Non-Adiabatic Wall Effects on Transonic Shock/Boundary layer Interaction", AIAA paper 83-1421, 1983.

9. Delery, J.M., "Shock Wave/Turbulent Boundary Layer Interaction and its Control", Prog. Aerospace Sci., Vol. 22, pp 209-280, 1985.

10. Green, J.E., Weeks, D.J. and Pugh, P.G., "Heat transfer as a source of spurious scale effects in subsonic and transonic wind tunnels", ARC 38182, May 1979.

11. Mabey, D.G., "Effects of Heat Transfer in Aerodynamics and Possible Implications for Wind Tunnel Tests", Progress in Aerospace Sciences, Vol. 27, No. 4, pp 267-303, 1991.

12. Raghunathan, S., Zarifi-Rad, F., and Mabey, D.G., "Investigations of the Effect of Model Cooling on Periodic Transonic Flow", AGARD Conference Proceedings, 507, Paper 26, 1992.

13. Baldwin, B.S. and Lomax, H., "Thin Layer Approximation and Algebraic Model for Separated Turbulent Flows", AIAA Paper 78-0257.

14. MacCormack, R.W., "Current Status of Numerical Solutions of the Navier-Stokes Equations", AIAA Paper 85-0032.

15. Van Leer, B., "Flux Vector Splitting for the Euler Equations", ICASE Report 82-30.

16. Mulder, W.A. and an Leer, B., "An Implicit Finite-Difference Algorithm for Hyperbolic Systems in Conservation-Law-Form", Journal of Computational Physics, Vol. 32, pp 87-110.

17. Cook, P.H., MacDonald, M.A. and Firmin, M.C.P., "Aerofoil RAE 2822-Pressure Distribution and Boundary Layer and Wake Measurements", AGARD-AR-138.

18. Maksymiuk, C.M. and Pulliam, T.H., "Viscous Transonic Airfoil Workshop Results Using ARC2D", AIAA Paper 87-0415.

19. Harris, C.D., "Two-Dimensional Aerodynamic Characteristics of the NACA0012 Airfoil in the Langley 8-Foot Transonic Pressure tunnel", NASA-TM-81927.

20. Pappas, C.C., "Measurement of Heat Transfer in the Turbulent Boundary Layer on a Flat Plate in Supersonic Flow and comparison with Skin Friction Results", NACA TN 3222.

21. Spalding, D.B. and Chi, S.W., "The Drag of a Compressible Turbulent Boundary Layer on a Smooth Flat Plate with and without Heat Transfer", Journal of Fluid Mechanics, Vol. 18, pp 117-143.

22. Back, L.H. and Cuffel, R.F., "Shock Wave/Turbulent Boundary Layer Interactions With and Without Surface Cooling", AIAA Journal, Vol. 14, No. 4, pp 526-532.

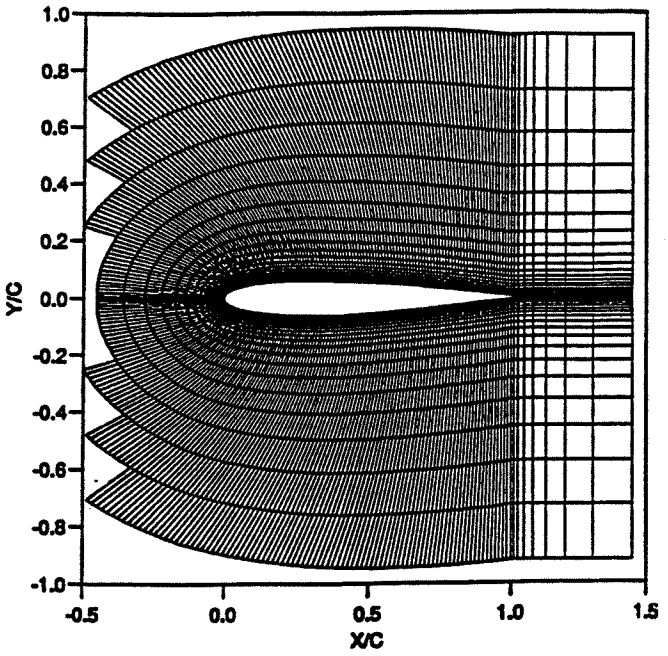

Fig. 1. C Grid

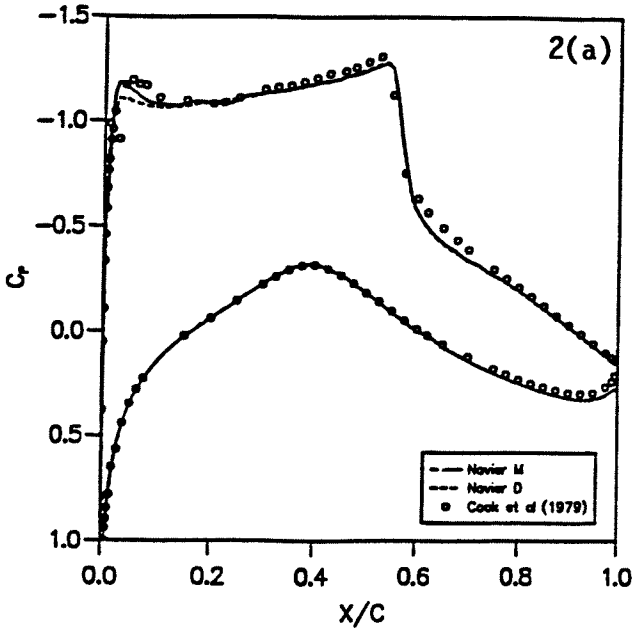

Fig. 2. Code Validation

(a) RAE 2822

M = 0.73, R = 6.5 x 10^6,

$\alpha = 2.79^0$, Transition fix 3%,

C Pressure distribution

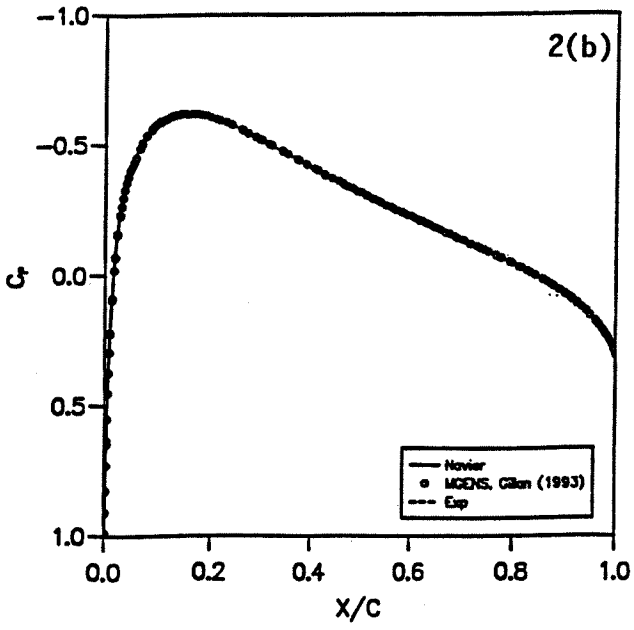

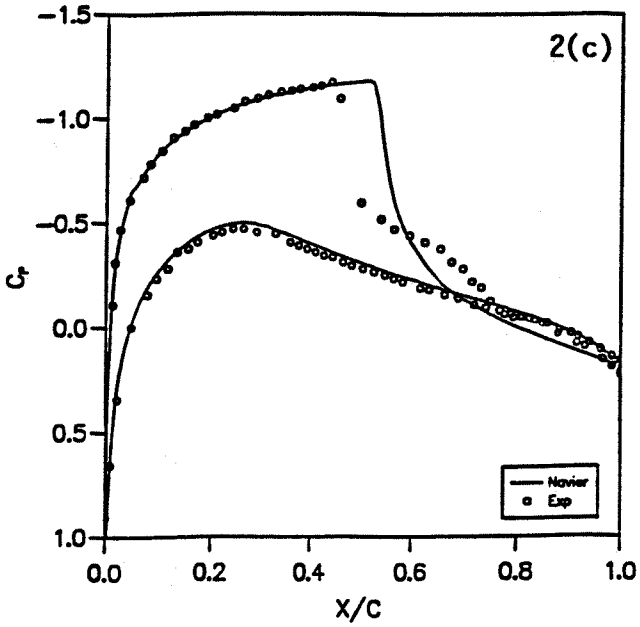

Fig. 2. (continued)

(b) NACA0012

M = 0.7, R = 9 x 10^6, $\alpha = 0$

Transition 5% C Pressure distribution

(c) NACA0012

M = 0.79, R = 9 x 10^6, $\alpha = 2.57$

Transition 5%, C Pressure distribution

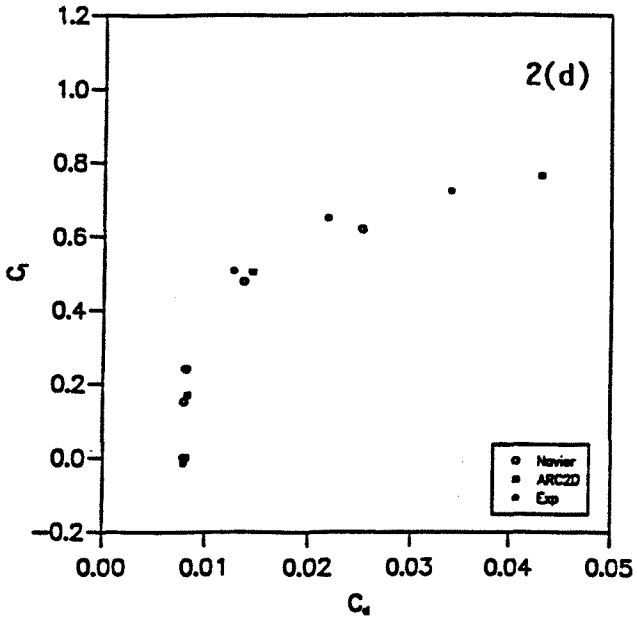

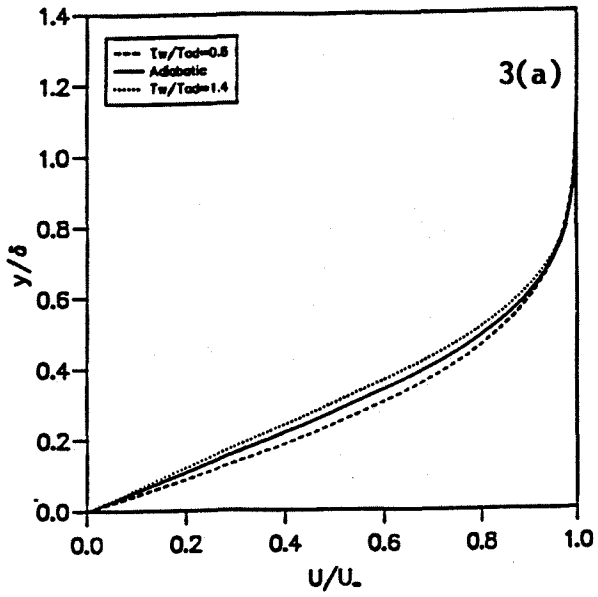

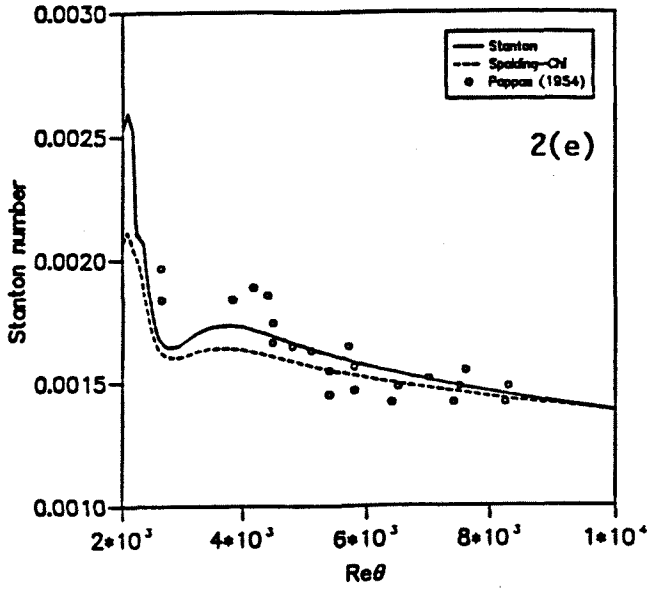

Fig. 2. (continued)

(d) Drag polar

NACA0012 M = 0.7,
R = 9 x 10^6

Transition 5% C

(e) Heat transfer on a flat plate

M = 1.69, R = 10^6, T_w/T_{ad} = 1.65

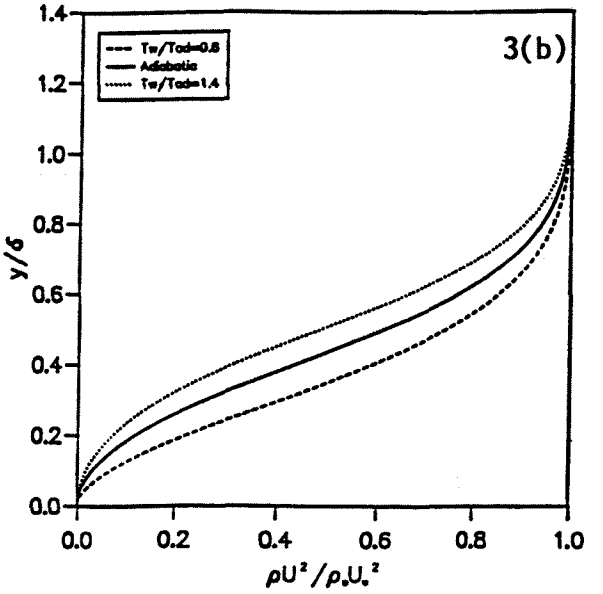

Fig. 3. Effect of heat transfer on laminar boundary layer

M = 0.5, R = 8 x 10^3,

(a) Velocity profile

(b) Momentum profile

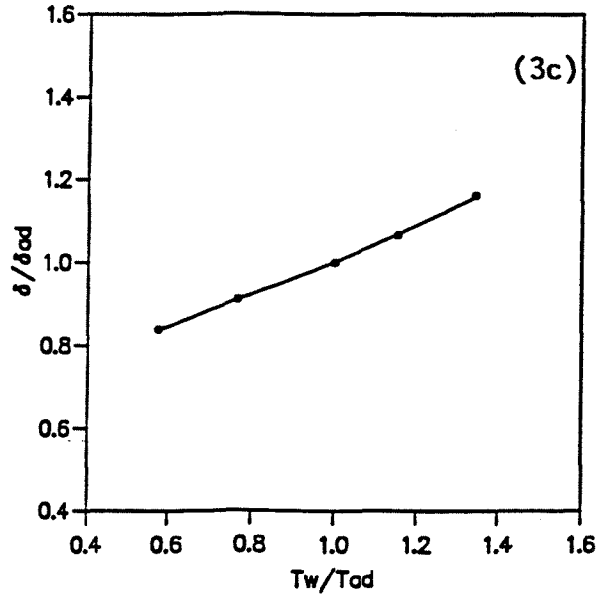

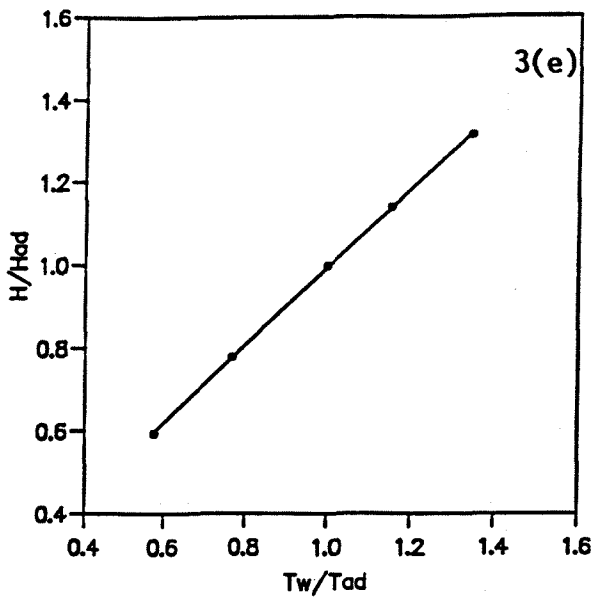

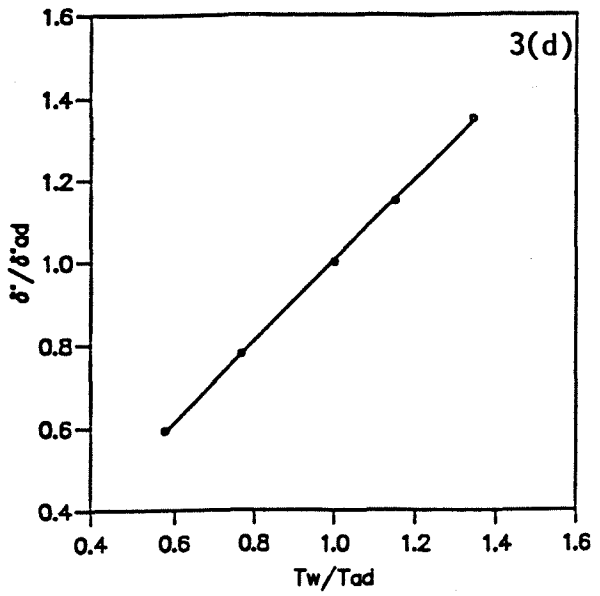

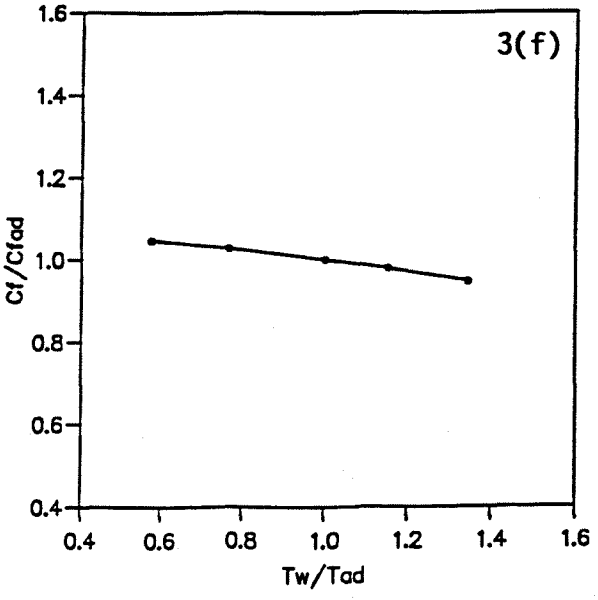

Fig. 3. (continued)

(c) Boundary layer thickness

(d) Displacement thickness

Fig. 3 (continued)

(e) Shape factor

(f) Skin friction

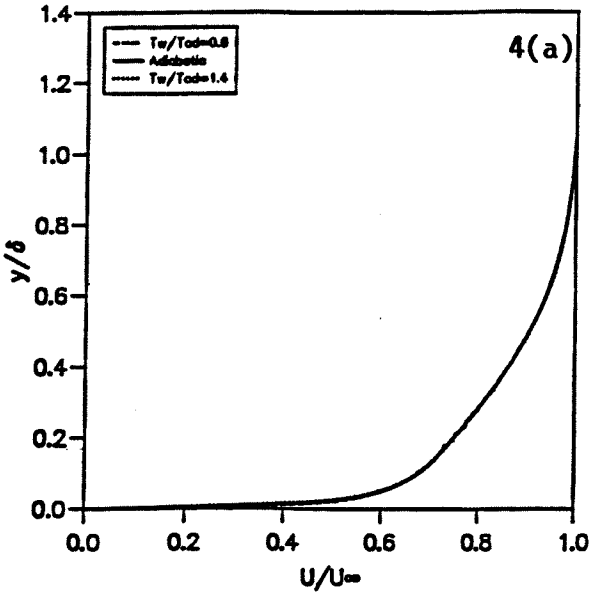

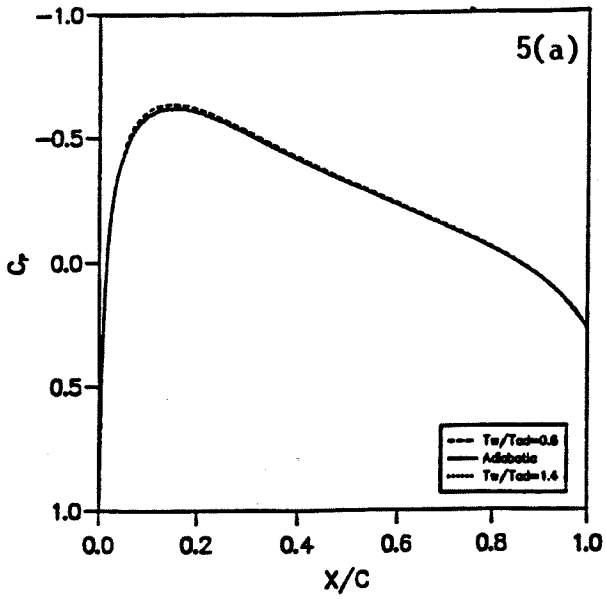

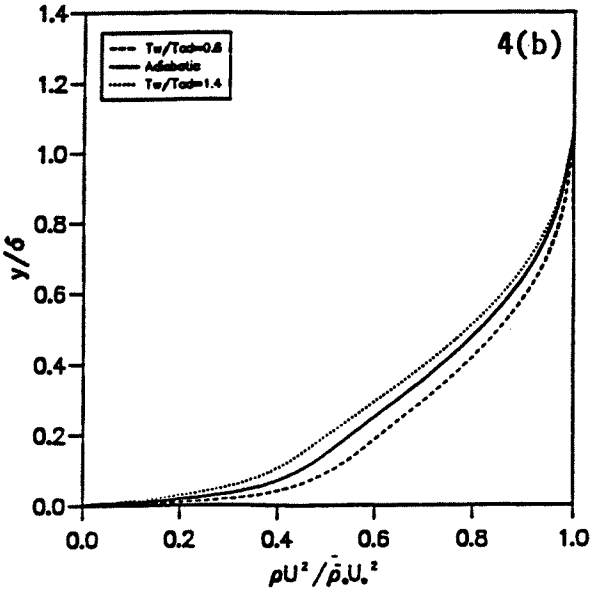

Fig. 4. Effect of heat transfer on turbulent boundary layers.
M = 0.7, R = 10^6

(a) Velocity profile

(b) Momentum profile

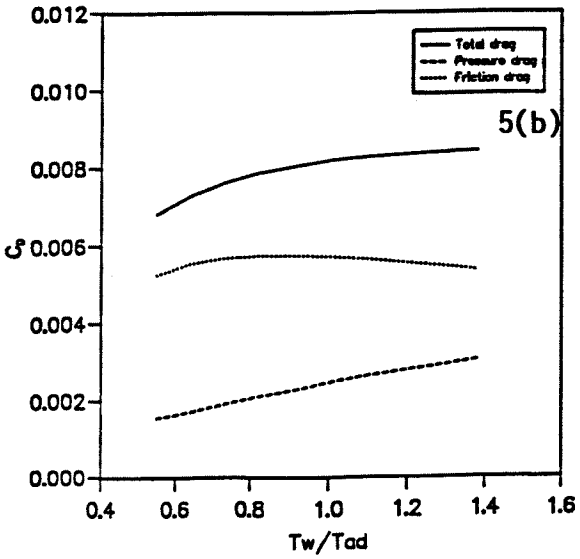

Fig. 5. Effect of heat transfer on NACA0012 profile at subcritical flow. M = 0.7, R = 9 x 10^6, α = 0. Transition 5% C

(a) Pressure distribution

(b) Drag

Fig. 5. (continued)

(e) Mach number profiles

(f) Momentum profiles

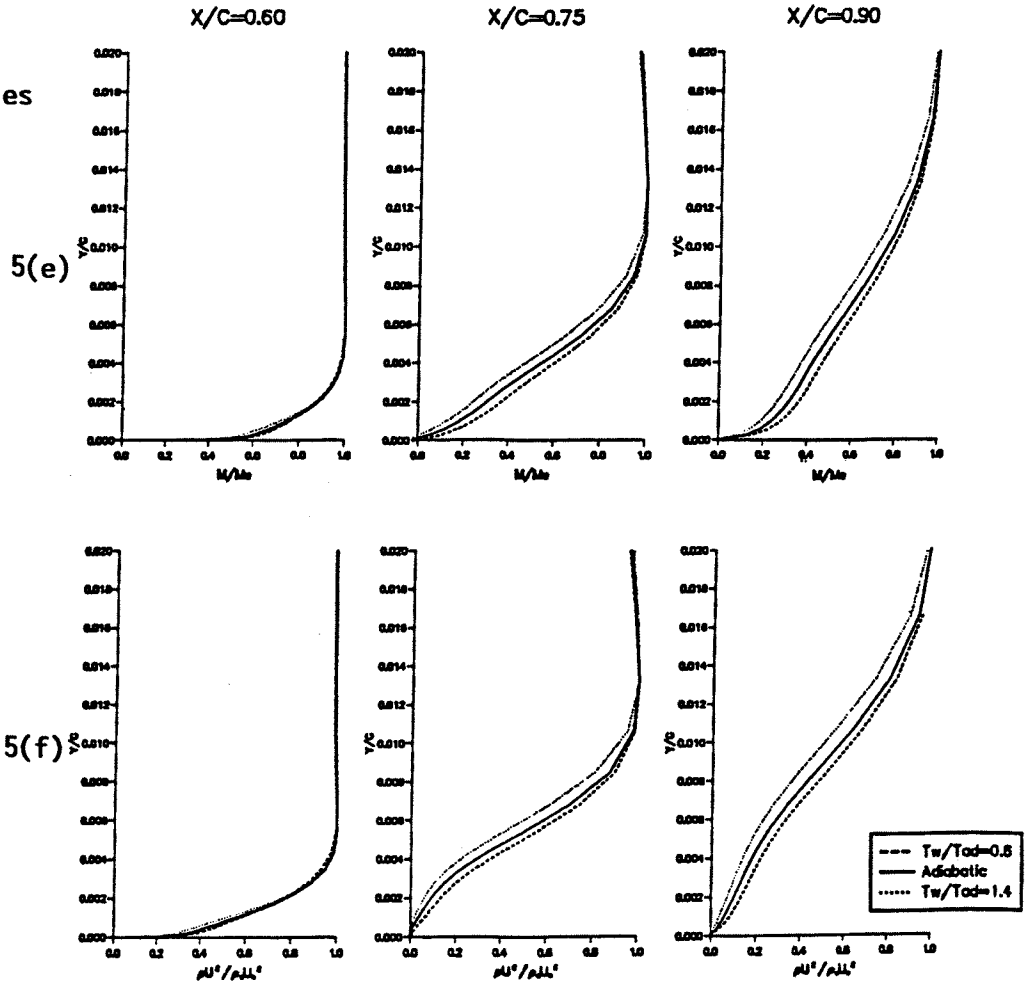

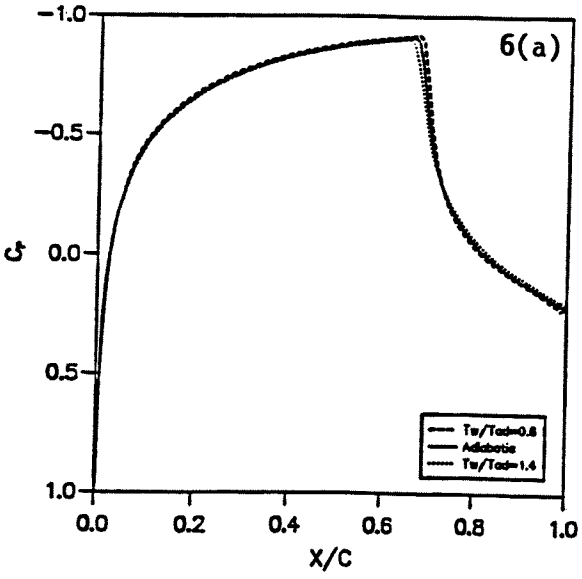

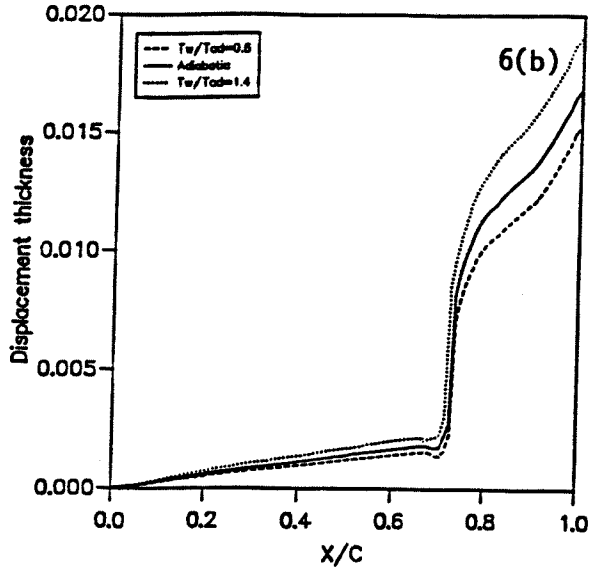

Fig. 6. Effect of heat transfer on transonic flow.

NACA0012, M = 0.85, R = 9 x 10^6, α = 0 deg.

Transition fix 5% C

(a) Pressure distribution

(b) Displacement thickness

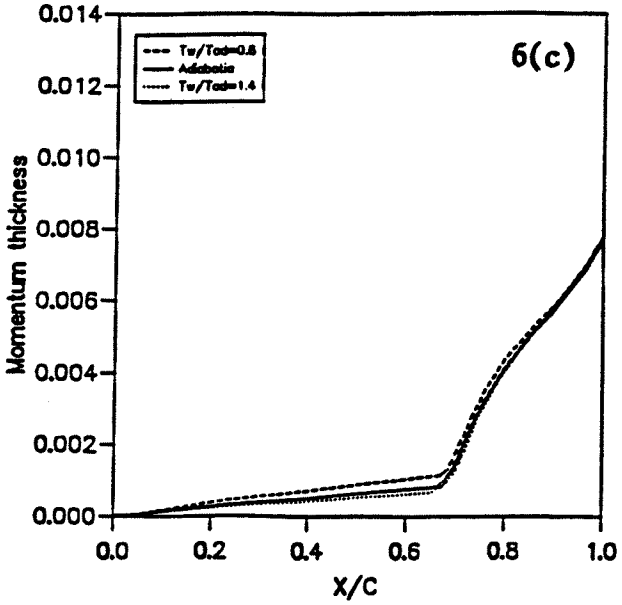

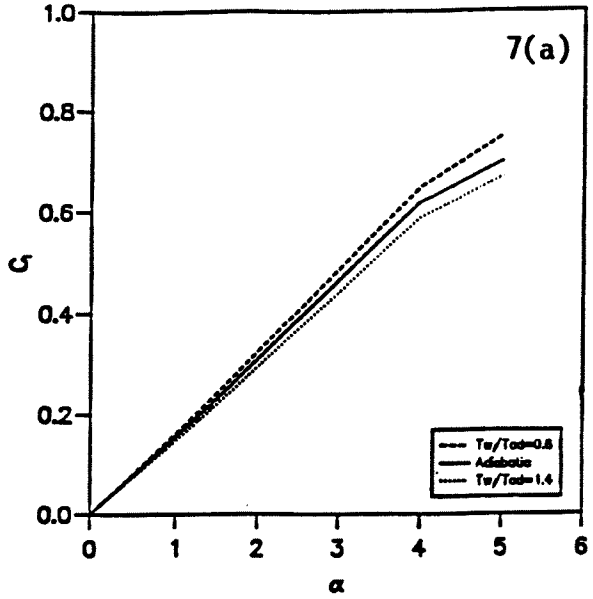

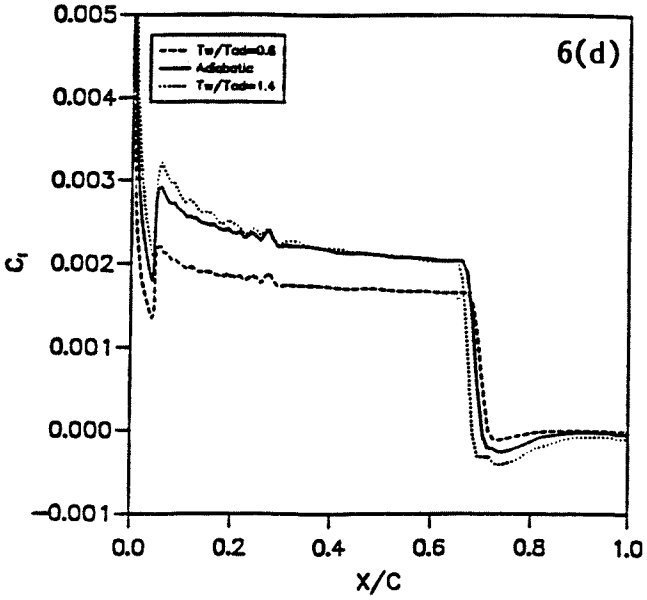

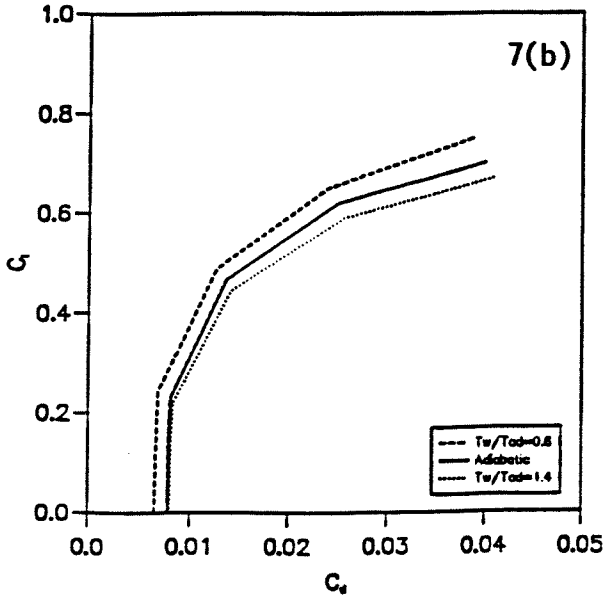

(c) Momentum thickness

(d) Skin friction

Fig. 7. Effect of heat transfer on aerodynamic forces.

NACA0012, M = 0.7 R = 9 x 10^6

Transition fix 5% C

(a) Lift

(b) Drag polar